Asteroid break-ups and meteorite delivery to Earth the past 500 million years

Fredrik Terfelt[a] **and Birger Schmitz**[a,b,1]

[a]Astrogeobiology Laboratory, Department of Physics, Lund University, 221 00 Lund, Sweden; and [b]Robert A. Pritzker Center for Meteoritics and Polar Studies, Negaunee Integrative Research Center, Field Museum of Natural History, Chicago, IL 60605

Edited by William F. Bottke, Southwest Research Institute, and accepted by Editorial Board Member Donald E. Canfield April 21, 2021 (received for review October 7, 2020)

The meteoritic material falling on Earth is believed to derive from large break-up or cratering events in the asteroid belt. The flux of extraterrestrial material would then vary in accordance with the timing of such asteroid family-forming events. In order to validate this, we investigated marine sediments representing 15 time-windows in the Phanerozoic for content of micrometeoritic relict chrome-spinel grains (>32 µm). We compare these data with the timing of the 15 largest break-up events involving chrome-spinel–bearing asteroids (S- and V-types). Unexpectedly, our Phanerozoic time windows show a stable flux dominated by ordinary chondrites similar to today's flux. Only in the mid-Ordovician, in connection with the break-up of the L-chondrite parent body, do we observe an anomalous micrometeorite regime with a two to three orders-of-magnitude increase in the flux of L-chondritic chrome-spinel grains to Earth. This corresponds to a one order-of-magnitude excess in the number of impact craters in the mid-Ordovician following the L-chondrite break-up, the only resolvable peak in Phanerozoic cratering rates indicative of an asteroid shower. We argue that meteorites and small (<1-km-sized) asteroids impacting Earth mainly sample a very small region of orbital space in the asteroid belt. This selectiveness has been remarkably stable over the past 500 Ma.

meteorite delivery | chrome spinel | asteroid break-up | Phanerozoic history

Until recently, almost nothing was known about the flux rates and types of meteorites and micrometeorites that fell on Earth in deep time (before circa 1 Ma). Meteorite falls are rare and meteorites weather and decay rapidly on Earth's surface, making it a challenge to reconstruct ancient fluxes. Most meteorite types, however, contain a small fraction (∼0.1 to 0.3%) of very resistant spinel minerals that survive weathering and can be recovered by acid-dissolution of large samples (100 to 1,000 kg) of slowly deposited sediments of any age (1) (Fig. 1). Over the past years we have systematically searched for relict extraterrestrial spinel grains in sediments from different time windows of the Phanerozoic Eon in order to establish the first paleoflux record for meteorites to Earth (2–5). Such information is important because variations in the flux may potentially be related to astronomical events, like break-up events leading to the formation of major asteroid families in the asteroid belt or major cratering events on large asteroids, the Moon, or Mars (6, 7). More speculatively, subtle perturbations of the solar system (e.g., by nearby passing stars or chaos-related transitions in planetary orbits) could also affect from where in the solar system meteoritic matter originates. In different parts of the solar system, different types of material dominate (8) and therefore potential changes in the loci of meteorite origins may be detected by a paleoflux record. Here we add to the 11 previously studied windows, results from 4 crucial time windows: 2 in the Cambrian, our oldest time windows studied, and 2 in the Jurassic (Dataset S1). The latter two windows establish, together with the previous data, a high-coverage record for the past 170 Ma. Here, we also add data for one of our previously studied windows in the Late Cretaceous (5). The 15 time windows represent data obtained by acid-dissolution of in total 8,484 kg of sedimentary limestone about equally distributed over the windows (Table 1 and *SI Appendix*, *SI Text* and Figs. S1–S4). Each time window represents several 100-kg-sized samples collected over a stratigraphic interval corresponding to an ∼1- to 5-Ma period.

The variations in the flux of micrometeorites and meteorites to Earth is today generally described by the collisional cascading model, where large break-up events generate new fragment populations that feed the inner solar system with material for extended time periods, but gradually starve out due to collisional and dynamical evolution (6, 9, 10). Here we assess the validity of this meteorite delivery mechanism by comparing the extraterrestrial chrome-spinel flux in our time windows studied (Table 1) with the timing of the break-up events in the asteroid belt during the Phanerozoic involving asteroids that contain large (>32 µm) chrome-spinel grains (11–14) (Fig. 2). Primarily, asteroids of the spectral S- and V-types contain abundant chrome-spinel grains like those used in our reconstructions. There were also large break-up events involving other types of asteroids, but micrometeorites from such events would not give a signal in our chrome-spinel approach. These events, however, could leave a signal in the asteroid cratering rate on Earth, as well as in reconstructions of the extraterrestrial ^{3}He distribution in sedimentary strata or in the K-Ar gas retention ages of meteorites that have fallen on Earth in recent times. Thirty-one identified chrome-spinel–bearing asteroid families formed in the Phanerozoic (11, 12). All of these families are of the S-type. For the V-type asteroids we know of only one, or possibly two, events that may have led to an increase in the flux of material to Earth, but these are cratering rather than break-up events.

Significance

The standard view of meteorite delivery to Earth is that of the cascading model where large asteroid break-ups generate new fragment populations that feed the inner solar system with material for extended time periods. Our investigated time windows, stretching from the Cambrian to the present, do not support this model. In fact, of 70 major family-forming break-ups the past ∼500 Ma, only 1 appears to have given rise to a strongly enhanced flux to Earth. We argue that meteorites and small asteroids delivered to Earth in deep time are not primarily linked to the sequence of asteroid family-forming events. Another, as yet unknown, delivery process appears to be associated with a very restricted region in the asteroid belt.

Author contributions: F.T. and B.S. designed research, performed research, contributed new reagents/analytic tools, analyzed data, and wrote the paper.

The authors declare no competing interest.

This article is a PNAS Direct Submission. W.F.B. is a guest editor invited by the Editorial Board.

[1]To whom correspondence may be addressed. Email: birger.schmitz@nuclear.lu.se.

This article contains supporting information online at https://www.pnas.org/lookup/suppl/doi:10.1073/pnas.2020977118/-/DCSupplemental.

Published June 7, 2021.

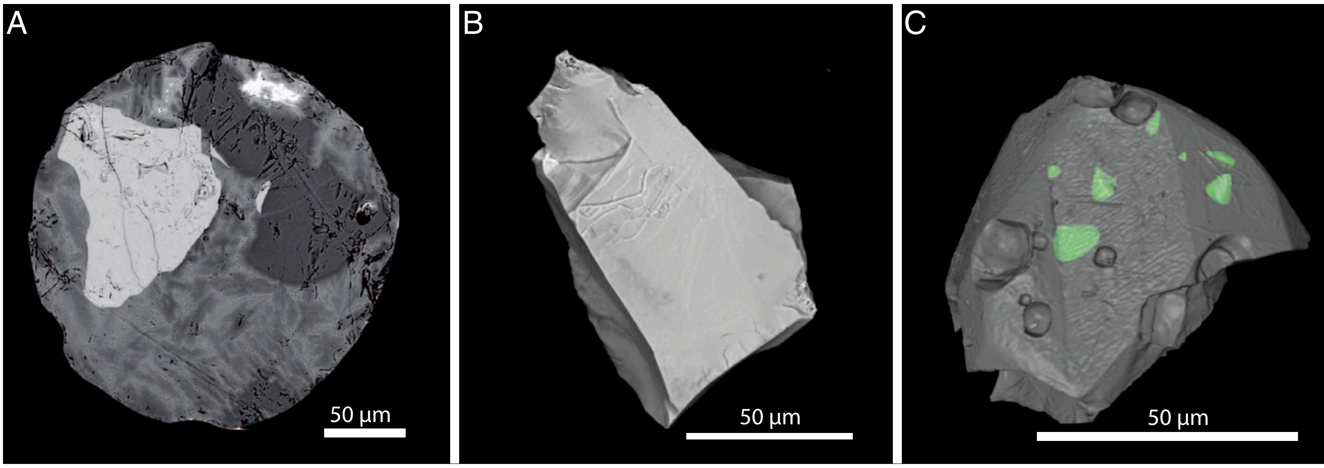

Fig. 1. Extraterrestrial chromite grains. (*A*) Recently fallen micrometeorite recovered in the Sør Rondane Mountains in East Antarctica (18). The backscattered electron image highlights a large (>63 μm) relict chromite grain (light gray) in a porphyritic olivine spherule. This relict chromite grain is angular, with limited indication of melting during atmospheric passage. (*B*) Extraterrestrial chromite grain recovered from mid-Ordovician marine limestone at Hällekis in southern Sweden. (*C*) Chromite grain from Farmington L5 ordinary chondrite with microtomographic three-dimensional reconstruction of original olivine and pyroxene inclusions highlighted in green. Silicate inclusions in chromite grains can be up to 400-μm^3 large, and used for detailed classification of precursor meteorite type.

Around 1 to 1.7 Ga ago the 500-km-sized Rheasilvia basin formed on the south pole of 4 Vesta by the impact of an ∼40-km-sized body. Possibly, there was also a second, later lower-energy impact of an ∼20-km-sized body on 4 Vesta, but the claim is ambiguous (15–17). Following the cascading concept laid out above, at least the 15 largest family-forming break-up events (with more than ∼500 members) presented in Fig. 2 should have produced large amounts of fine dust that would have reached Earth a few hundred thousand to a few million years later (Fig. 2). The robustness of our chrome-spinel data varies between different time windows, but we are confident that the present “first-order” dataset supports our main conclusions. The validity of our approach is supported by the high level of reproducibility of results for the same time windows at different sites in China, Russia, and Sweden. For example, the results for the mid-Ordovician window just before the L-chondrite parent body (LCPB) break-up as registered at Lynna River in Russia and Hällekis in Sweden, localities 1,100-km apart on the same paleocontinent, are very similar (Table 1 and *SI Appendix*, Table S1) (18). Previous research has shown that sediment-dispersed chrome-spinel grains mainly originate from unmelted micrometeorites in the size range 30 to 2,000 μm (1, 4, 18). The flux in this size fraction has been shown to correlate

Table 1. Overview of time-windows studied and their content of extraterrestrial chrome spinel

Time window	Ma	Kilograms of rock	EC^{32}	OtC -V^{32}	EC/OtC -V^{32}	EC^{63}	OtC -V^{63}	EC/OtC-V^{63}	EC^{32} m^{-2} ka^{-1}	EC^{63} m^{-2} ka^{-1}
Early Paleocene (26)	∼66–61	843	74*	39*	1.9	12	5	2.4	1.3	0.15
Late Cretaceous (5)†	∼92–91	944	108	45	2.4	5	3	(1.7)	2.9	0.25‡
Late Cretaceous (5)	∼94–92	432	50	4	12.5	9	0	>9.0	2.9	0.25‡
Early Cretaceous (57)	∼117–103	689	217	73	3.0	10	5	2.0	2.7	0.12
Early Cretaceous (2)	∼145–133	1652	79	25	3.0	2	2	(1.0)	3.0	(0.08)
Middle Jurassic†	∼166–164	214	n/a	n/a	n/a	142	35	4.1	n/a	0.17
Middle Jurassic†	∼168–166	609	66§	9§	7.3	44	20	2.2	4.7§	0.54
Late Devonian (4)	∼374–372	898	n/a	n/a	n/a	46	12	3.8	n/a	0.45
Late Silurian (3)	∼426–424	321	154	13	11.9	10	1	10.0	4.8	0.31
Middle Ordovician (58)	∼463–462	51	n/a	n/a	n/a	23	4	5.8	n/a	3.8
Middle Ordovician (3)	∼466–465¶	102	>7,000	n/a	n/a	474	8#	59#	>429	29
Middle Ordovician (2, 10)	∼467–466‖	285	189	n/a	n/a	26	20	1.3	1.2	0.16
Middle Ordovician (18)	∼467–466‖	791	228	49	4.7	15	14	1.1	2.4	0.16
Late Cambrian†	∼500–499	341	159**	44**	3.6	41	11	3.7	2.9	0.48
Late Cambrian†	∼503–502	312	129	42	3.1	18	15	1.2	1.7	0.23
Grand total	∼503–61	8,484	>8,453	343	n/a	877	155	n/a	n/a	n/a

EC^{32} and OtC-V^{32} = EC and OtC-V grains 32- to 63-μm large. EC^{63} and OtC-V^{63} = EC and OtC-V grains 63- to 355-μm large. Values in parentheses based on only few grains.
*From 633 kg.
†This study.
‡Flux based on the 14 grains from both sample sets in the Late Cretaceous.
§From 106 kg.
¶Post-LCPB.
#All OtC-V grains likely from unequilibrated ordinary chondrites.
‖Pre-LCPB.
**From 217 kg.

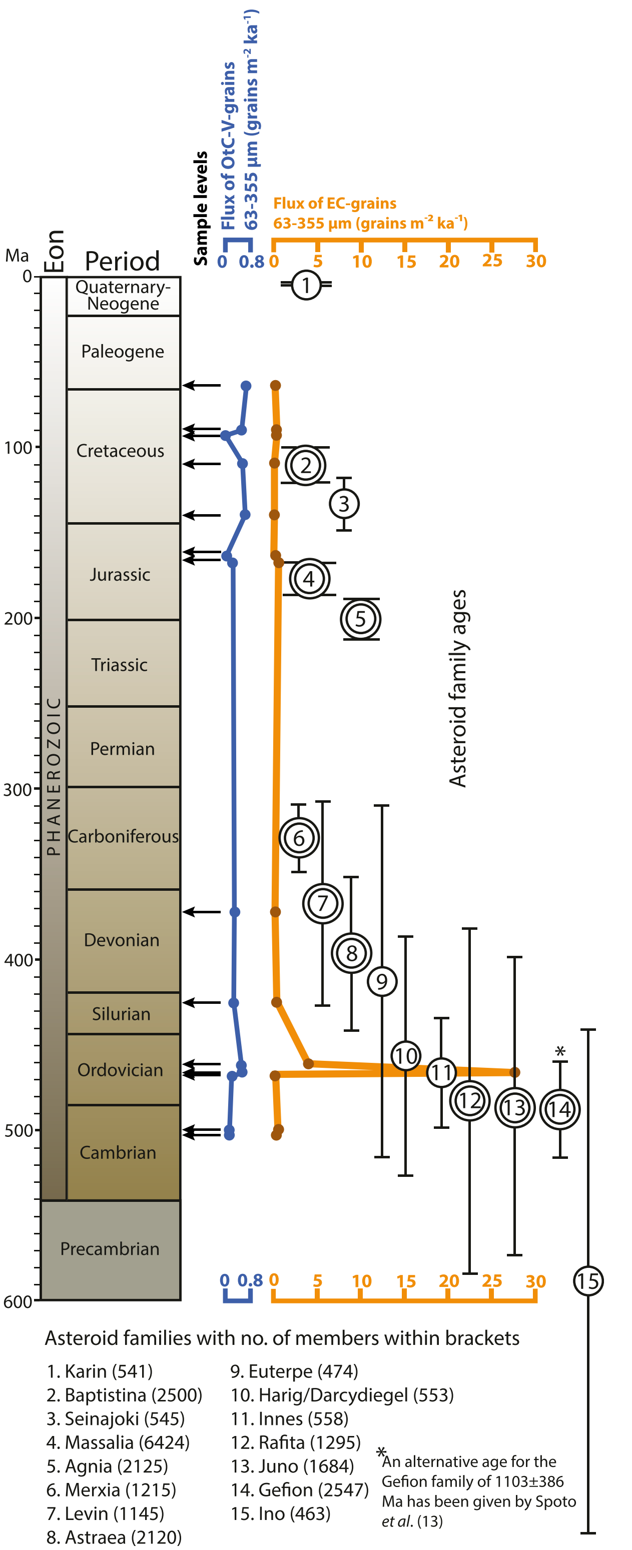

Fig. 2. Extraterrestrial flux data from 15 time windows in the Phanerozoic plotted against 15 asteroid family ages. Only asteroid families of the types known to contain abundant large chrome-spinel grains are plotted. Thirty-one asteroid families contain large chrome-spinel grains formed in the Phanerozoic, but only the 15 largest (>500 members) are plotted here. The largest families (>1,000 members) are highlighted with double circles. Note the close to constant flux of ordinary chondritic micrometeorites through the Phanerozoic with the conspicuous exception of the mid-Ordovician peak following the L-chondrite parent body break-up ~466 Ma (56). The asteroid family ages and errors follow Reiners and Turchyn (11), as well as the number of family members except for Seinajoki, where we follow Spoto et al. (13). The spectral type of the families is based on Reiners and Turchyn (11), except for Seinajoki, Levin, and Harig/Darcydiegel, where information is from Spoto et al. (13).

with the flux of larger meteorites (e.g., in the size interval 1 to 20 cm).

Results

Our chrome-spinel data show an intriguing pattern where the LCPB break-up 466 Ma ago constitutes a conspicuous anomaly during a 500 million y more-or-less constant ordinary chondritic flux. Throughout the Phanerozoic, except following the LCPB event, the flux of ordinary chondritic chrome spinel appears to have been stable in the range of ~0.1 to 0.5 grains (>63 µm) m^{-2} kyr^{-1}. During circa 2 million y following the LCPB event, the flux increases by a factor of ~100 to 300 and the chrome-spinel assemblages are almost entirely (>99%) made up of L-chondritic grains (18). The increased flux of micrometeorites from this event tailed off, but continued into Silurian times, when it finally reached background values after some 40 million y (3) (Fig. 2). Even today, this break-up is the source of almost one-third of all meteorites falling on Earth. In all other time windows, the total flux lies at background levels and the ratios between grains from equilibrated ordinary chondrites (EC grains) and other chrome-spinel bearing meteorite types (OtC-V grains) show that ordinary chondrites dominated the flux among chrome-spinel–yielding meteorite types (Table 1). The OtC-V grains do not have the typical equilibrated ordinary chondritic composition, but have high vanadium content that generally distinguishes extraterrestrial from terrestrial spinels (see *Materials and Methods* for a detailed discussion). For 2 of our 15 time windows we also have three oxygen isotopic data for the OtC-V grains recovered, allowing a more precise characterization of their origin. In the oldest Early Cretaceous window, about one-third of the OtC-V grains have an oxygen isotopic composition indicative of the howardite, eucrite, diogenite (HED) types of meteorites (2). Another third of the grains represent unequilibrated ordinary chondritic grains, and the remainder originate from primitive (e.g., winonaites, lodranites, acapulcoites) or ungrouped or anomalous achondrites.

Previously, we have reported a rather low (~1.1) EC/OtC-V ratio in the 63- to 355-µm fraction just before the LCPB break-up (10). The oxygen isotopic studies of the mid-Ordovician OtC-V grains show that a substantial fraction of them originate from different types of primitive achondrites rarely seen in the present flux (10). We see similar low EC/OtC-V ratios also in some of the other time windows, but the flux of EC grains remains stable at background levels and ordinary chondrites still dominate (Fig. 2 and Table 1). In the chrome-spinel assemblage from the mid-Ordovician before the LCPB break-up, we noted an HED/ordinary chondritic ratio a factor two to five higher than in today's flux. This was inferred to reflect a residual signature after the formation of the Rheasilvia basin at ~1 to 1.7 Ga ago (17). This interpretation was reasonable in light of the great uncertainties in the estimated age of the Rheasilvia basin. The HED meteorites represent the second most-common group in the collections of recently fallen meteorites (representing ~6% of all meteorite falls) (19), and they appear to have held this position through most of the Phanerozoic. Without detailed oxygen isotopic studies for most of the OtC-V grains in our 15 time windows, considerable uncertainty exists in the details regarding the origin of these grains. Our data, however, clearly show that none of the time windows has registered any major achondritic micrometeorite flux increases following a large-scale family-forming or cratering event during the Phanerozoic.

https://doi.org/10.1073/pnas.2020977118

Discussion

Time Windows and Break-up Events. Arguably, our sampling coverage in the Phanerozoic is not all-encompassing. The Carboniferous to early Jurassic constitutes an ~190-million-y stretch without chrome-spinel data and an asteroid disruption event during this time would probably go unnoticed. However, only one major break-up event occurred during this time: the Merxia asteroid family event in the Carboniferous (Fig. 2). Any break-up after the Triassic would have been recorded in our sampling windows considering the tailing off time of tens of millions of years after the first arrival of dust from a major parent-body break-up. A feasible argument for the discrepancy between asteroid fragmentation events and observed sediment-dispersed chrome-spinel data may be due to the size and the degree of fragmentation of the parent body. Of the six largest chrome-spinel–bearing asteroid families only one, the Massalia family, is younger than 500 million y (Fig. 2). This cratering/disruption event took place during the mid-Jurassic; however, no obvious traces of the event were found in the mid-Jurassic to early Cretaceous time windows (Fig. 2). A possible explanation is that the Massalia family is a cratering family with a typical mass concentration in one or a few members (20). Its two largest members (150 km and 7 km in diameter) constitute 99% of the total mass of its 6,424 members (20), which demonstrates that this disruption was rather limited and probably did not produce enough dust to affect the flux rate on Earth.

On the other hand, the Baptistina asteroid family, comprising 2,500 members, likely formed in mid-Cretaceous times (Fig. 2) and is considered to have an LL-chondritic composition (21, 22). The Cretaceous happens to be our most densely sampled period, but there are no signs at all of a significantly enhanced flux of LL-chondritic chrome-spinel grains in any of our Cretaceous samples. Based on family-member orbital backtracking, other ages, in the range 210 to 140 Ma, have been proposed for the Baptistina break-up (23), but nor in the Jurassic samples from approximately 170 Ma is there a significant (greater than a factor of two) enhancement in the flux of LL-chondritic grains.

Considering the dynamical age of 950 (+200/−170) Ma for the formation of one of the largest asteroid families, the LL-chondritic Flora family (12, 24), we expected to see a significant enhancement of LL-chondritic grains in our two Cambrian time windows. The Flora family has 14,000 members and formed close to the $\nu6$ resonance, fulfilling the assumed requirements to be a major meteorite provider 500 Ma (12). In today's world the L chondrites still represent the most abundant type of meteorite falling on Earth 466 Ma after the LCPB break-up. By analogy, one would therefore have expected that in the Cambrian, ~400 Ma after the large Flora break-up, LL chondrites would instead have dominated among the ordinary chondrites, but there is no obvious enhanced LL-chondritic signal in any of the Cambrian windows compared to other younger time windows (Fig. 3, Table 1, and *SI Appendix*, Table S1).

Instead, H chondrites clearly dominated the flux in the Cambrian, making up 62 to 71% of the ordinary chondrites falling. There is no significant enhancement in the total flux of ordinary chondritic grains in the Cambrian. In the oldest Cambrian window, LL-chondritic grains make up 18% of the ordinary chondrite flux, and 3 million y later LLs represent 14%. This is similar to 12% in today's flux and to values around 6 to 13% through most of the Phanerozoic (Fig. 3 and *SI Appendix*, Table S1). Our results indicate that the LL chondrites arriving on Earth today may originate from the same region in the asteroid belt as the H and L chondrites rather than from the Flora family region. Notably, in the mid-Ordovician just before the LCPB break-up, the LL chondrites represent almost a third of the flux (30%). The mid-Ordovician windows also show other unusual features such as the common large (63 to 250 μm) grains from different types of primitive achondrites in pre-LCPB strata (10) and a fossil primitive achondritic

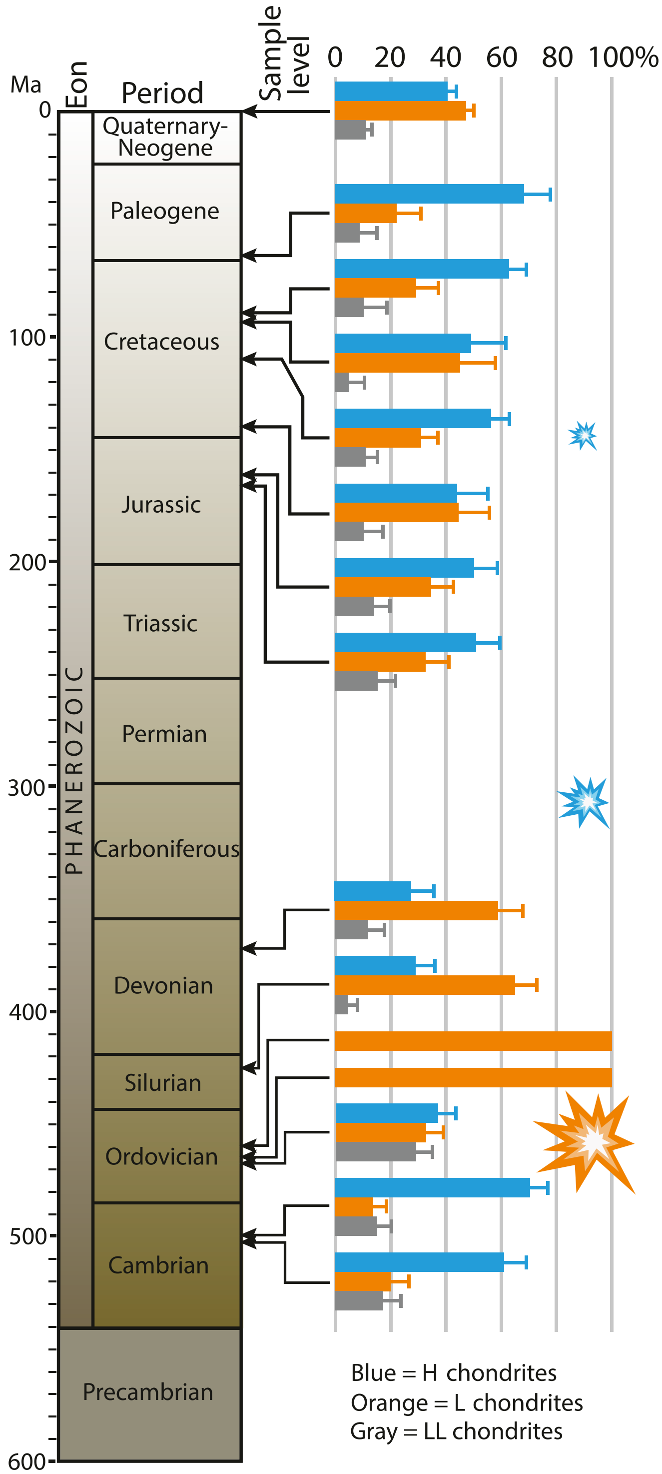

Fig. 3. Variations through the Phanerozoic in the relative proportions of the three groups of ordinary chondrites based on chrome spinel. Percentages of H, L, and LL chondrites among ordinary chondrites. The large orange star indicates the timing of the major break-up of the L-chondrite parent body at ~470 Ma based on K-Ar isotopic ages of recently fallen L-chondrites (28–31). The two smaller blue stars illustrate two possible smaller impact events on the H-chondrite parent body according to K-Ar data of recently fallen H chondrites (31) and data in the present study. The plot is based on both the small (32 to 63 μm) and the large (>63 μm) fraction of EC grains. Percentages are based on TiO_2 values corrected for compositional overlap between the groups. Error bars indicate 1σ uncertainties. See also *SI Appendix*, *SI Text* and Tables S1 and S2.

meteorite of a type not previously known among Earth's meteorite types (25) in post-LCPB strata.

Another conundrum arising from our data is that L-chondritic micrometeorites were commonly falling on Earth even before the LCPB event both in the Cambrian and the mid-Ordovician (Fig. 3, Table 1, and *SI Appendix*, Table S1). In assemblages representing the time about 1 million y before the LCPB break-up the L chondrites already constitute about one-third of the ordinary chondrites with a flux rate on the same order of magnitude as the Phanerozoic background flux. In the Cambrian time windows, we see some of the lowest L-chondritic percentages of the Phanerozoic, 12 to 17%, but also in the early Paleocene, ~66 to 61 Ma ago, are such low values recorded (26).

In essence, our data show that the meteorite flux has been remarkably stable over time and, except for the LCPB event, none of the asteroid break-ups considered appear to have led to major changes in the meteorite flux to Earth. In particular, the absence in our micrometeorite records of any signatures of the two large Flora and Baptistina break-up events, places strong doubts on the validity on present ideas that large family-forming events would have major effects on the delivery of meteoritic material to Earth.

Impact Cratering Record, K-Ar Gas Retention Ages, and ^{3}He Data. Based on the chrome-spinel data from the investigated time windows, we argue that asteroid disruption events of such magnitude as to give an order-of-magnitude or more increase in the meteorite flux to Earth over millions of years are exceedingly rare and may have happened only once (after the LCPB event) during the past 500 million y. Admittedly, our chrome-spinel data only give insights about events involving S- and V-type asteroids; however, clues about the flux effects of break-ups involving other types of asteroids as well (e.g., C, X, CX), with only rare large chrome-spinel grains, can be gained from three other records: 1) the age distribution of Earth's impact craters, 2) the K-Ar gas retention ages of nonfragile types of meteorites that have fallen on Earth in recent times, and 3) ^{3}He profiles across marine sedimentary sections. Below we summarize that our interpretations based on chrome spinels about asteroid break-ups and meteorite delivery to Earth are consistent with and supported by these three entirely independent data records.

In compilations of the ages of the ~200 impact craters known on Earth, there is only one resolvable "peak" in crater abundances indicative of an asteroid shower (27). This is a one order-of-magnitude higher number of craters ~470 to 440 Ma compared to other equivalent Paleozoic time bins. Most of these "excess" craters are small, 1 to 10 km in diameter, which is consistent with an origin of a shower of small asteroids from the broken-up ~150-km-large LCPB in the asteroid belt at ~466 Ma. Similarly, in the record of K-Ar gas-retention ages of many types of recently fallen meteorites studied, only one major break-up event is recorded during the Phanerozoic, the break-up of the LCPB ~470 Ma (28–31).

The K-Ar isotope system measures the time when collisional shock effects reset the K-Ar "isotopic clock" by Ar degassing. The K-Ar ages of meteorites are considered to reflect large, catastrophic events of sufficient energy to completely degas a major asteroid parent body. Almost all meteorite types have kept their Ar since when the solar system was young, but the two most common types of meteorites, the L and H chondrites, mostly show Phanerozoic K-Ar ages (31). The L chondrites show one prominent K-Ar age spike ~470 Ma, reflecting one major collisional event, whereas the H-chondrite parent body appears to have experienced a series of smaller collisional events throughout the Phanerozoic (31). The latter circumstance is registered in our data by recurrent returns to H-chondrite dominance among the ordinary chondritic micrometeorites that fell, and not by any major spike in the flux like for the L chondrites ~466 Ma (Fig. 3). Our interpretation of the Phanerozoic chrome-spinel distribution is also consistent with reconstructions of the extraterrestrial ^{3}He content in sedimentary sections. This ^{3}He is considered to represent the most fine-grained (<10-μm) fraction of the extraterrestrial dust arriving on Earth (32). The sedimentary record representing the past 100 Ma has been scanned in great detail for ^{3}He, providing evidence of five anomalies: three in the Late Cretaceous, and two in Cenozoic strata (32–34). However, the anomalies only reflect minor increases in the flux of ^{3}He-carrying dust, typically by a factor two to five over periods of 0.1 to 2 Ma. We have searched three of the ^{3}He-rich intervals for extraterrestrial spinels (>32 μm), but could not detect any micrometeorite flux increases larger than a factor of two (5, 26, 35, 36).

In comparison, in mid-Ordovician strata at the stratigraphic level where the first abundant L-chondritic micrometeorites from the LCPB break-up arrive, there is an increase in the extraterrestrial ^{3}He content by a factor of 240, but apparent gas loss in sediments this old suggests that the true increase may have been even higher (18). In essence, the available data from four different parameters—chrome spinel, impact-crater ages, K-Ar ages of meteorites, and sedimentary ^{3}He—only indicate a single break-up or cratering event (the LCPB break-up) during the Phanerozoic that led to an increase in the flux of meteorites to Earth at the order-of-magnitude level.

The Astronomical Data. Dynamical backtracking studies of the orbits of asteroid family members of all spectral types indicate about 70 major family-forming break-ups the past ~500 Ma (11–14), but our data from the geological record indicate that only one break-up event had any major effects on the accretion of meteorites and small asteroids on Earth. In the light of this, questions arise regarding the validity of the generally accepted delivery mechanisms of micrometeorites, meteorites, and asteroids to Earth. The delivery model is rather complex and is quite different for dust and micrometeorites compared to large bodies, such as meteorites and asteroids. For the large bodies a chain of events is envisioned, including (sequential): collisional break-up, semimajor axis drift induced by Yarkovsky effects (anisotropic heat emission that change the orbits of large objects), thin resonance influence of the eccentricity up to Mars-crossing status and, finally, hurling into an Earth-crossing orbit by a strong resonance (37). For small particles, the solar radiation pressure is believed to be the principal transport force (38, 39). Micrometeoroids (circa 10-μm to 2-mm large) are affected by the tangential component of the solar radiation known as the Poynting–Robertson drag, causing these fragments to coil into the inner solar system and the Sun (39). Therefore, according to theory, small fragments from break-up events in the asteroid belt can drift into Earth-crossing orbits without help from resonances on time scales of 0.1 to 10 Ma, depending on the distance and fragment size (4, 39).

The Provenance of Meteoritic Material Delivered to Earth. Although the ordinary chondrites make up as much as 87% of all recently fallen 63,000 meteorites documented (19), it is still a major conundrum from where in the inner to the middle asteroid belt they originate and why they so strongly dominate the recent flux (7, 8, 40–42). The fact that this dominance has prevailed for the past 500 Ma makes the issue even more elusive. Studies of the present asteroid belt indicate that 85% of all meteoroid debris in the inner asteroid belt is related to five major asteroid families: Flora, Vesta, Nysa, Polana, and Eulalia (43). Of these, the Flora family may be related to the least-common type of ordinary chondrites, the LL chondrites (41). However, none of the other four major families show a clear spectral relation to the abundant H or L chondrites falling on Earth today. A number of parent bodies/families have been proposed for the H and L chondrites, including asteroids Hebe, Juno, Agnia, Merxia, or the Koronis family for the H chondrites, and the Gefion or Ino families for L chondrites, but little agreement exists between different authors (44–49). The place of

https://doi.org/10.1073/pnas.2020977118

origin in the asteroid belt of the bulk of the ordinary chondrites represents a major enigma in meteoritics.

We argue that the present mode of meteorite delivery has been remarkably stable over the past 500 Ma, with the bulk of meteorites persistently originating from a rather restricted region of orbital space in the asteroid belt, but from where remains an enigma. It has been speculated that because most ordinary chondrites fall in the afternoon, their source region may be close to the 3:1 resonance (50). Spectral studies, however, show considerable diversity among asteroid types adjacent to the 3:1 resonance with no clear dominance of ordinary chondrites (51). Major asteroid break-up events in regions far away from resonances likely only result in more modest increases over shorter time scales in the flux of micrometeorites and meteorites to Earth. We know from cosmic-ray exposure (CRE) ages of recently fallen meteorites that the collisional cascade model is applicable on a smaller scale when variations in the flux of the different types of the ordinary chondrites are considered. Whereas K-Ar dates of meteorites reflect major degassing events, the CRE ages measure less energetic collisions when fragmentation creates pieces <1 m, the depth at which cosmic rays can penetrate (52). Recently fallen H, L, and LL chondrites show peak CRE ages of 7, 40, and 15 Ma, respectively, reflecting smaller break-up events successively sending meteorite showers to Earth (52). We note in our data that whereas the total flux of ordinary chondritic micrometeorites has been relatively stable during the past 500 Ma, except after the conspicuous LCPB event, the relations between the three different types of ordinary chondrites appear to vary with a turnover rate of a few to tens of millions of years (Fig. 3). This concurs with repeated smaller collisional events like those inducing different CRE ages of the recently fallen ordinary chondrites. The chrome-spinel approach ties Earth's geological record to the history of the asteroid belt and provides detailed information on orbital dynamics and processes in the asteroid belt not accessible through any other means.

Materials and Methods

Chrome-Spinel Separation. The present study is based on data from 2,828 extraterrestrial chrome-spinel grains 32- to 355-μm large. These grains were extracted from 8,484 kg of Phanerozoic limestone by means of acid dissolution. The extraction procedure is generally the same for all samples, however, the Cambrian, Jurassic and part of the Late Cretaceous data derive from new samples prepared for this study and a description of the chrome-spinel separation method for these follows in a step-by-step fashion. The limestone sample preparation was performed at the Astrogeobiology Laboratory, Lund University, Sweden. A total of 653 kg of Cambrian limestone, 823 kg of Jurassic limestone, and 397 kg of Late Cretaceous limestone were cleaned with a pressure washer to rid loose material and weathered rock. Subsamples of 95 to 110 kg of the clean rock were placed in 520 L plastic containers and submerged in 400 L of 6 M hydrochloric acid (HCl). After dissolution of the calcium carbonate (24 to 72 h), the residue was neutralized with sodium hydroxide (NaOH) and wet-sieved through a 32-μm mesh, thereafter the HCl-NaOH–sieving treatment was repeated once more to ensure complete $CaCO_3$ dissolution. The HCl-insoluble residue was then treated with 11 M hydrofluoric acid (HF) for 48 h with occasional stirring in order to dissolve siliciclastic minerals. After neutralization of the HF by means of repeated water decanting, the remaining material was dried and treated with 18 M sulfuric acid (H_2SO_4) for 12 h to dissolve hydroxide minerals, neutralized with NaOH, sieved at 32-μm mesh, and dried.

The dried residues from the Cambrian samples at this step contained vast amounts of pyrite and in order to dissolve this mineral, these samples were treated with 15.4 M nitric acid (HNO_3). The pyrite-free samples were then neutralized with NaOH, sieved through a 32-μm mesh, and dried. The dried remainder was treated with lithium heteropolytungstate dissolved in water (LST) at a relative density of 2.8 g cm^{-1} in order to remove organic material. The heavy liquid separates the material into a bottom-dwelling heavy fraction and a light fraction at the top of the liquid. The heavy fraction was physically separated from the light-weight fraction by freezing the bottom in liquid nitrogen, after which the liquid at the top (containing the light fraction) was poured off into a 32-μm mesh, washed, and burned in a furnace at 500 °C. The heavy fraction was thawed with water and divided into two size fractions (32 to 63 μm and 63 to 355 μm, respectively) and searched beneath a stereo microscope for opaque, black grains, which were picked with a fine brush and placed on a carbon tab on a glass slide for further investigation. The burned fraction was treated in the same way. The Jurassic and Cretaceous samples followed the same procedure, except for the HNO_3 treatment. Each process in the extraction procedure has been thoroughly tested on Ordovician extraterrestrial chrome-spinel grains in order to ensure that chemical or other treatment leave the grains unaffected. This has been carried out in a before-and-after fashion, where grains of different size fractions have been chemically analyzed and photographed prior to, and after a specific treatment. All steps in the treatment chain left all grains chemically and otherwise unaltered.

Elemental Analysis. Picked grains were analyzed semiquantitatively with a Bruker MinSVE energy-dispersive spectrometer mounted on a Hitachi TM 3030 Table Top scanning electron microscope to pinpoint grains with chrome-spinel composition. The confirmed chrome-spinel grains were mounted in epoxy resin and polished with 1-μm diamond paste. The polished grains were then coated with carbon and quantitatively analyzed for chemical composition with a calibrated Oxford INCA X-Sight energy-dispersive spectrometer with a Si detector, mounted on a Hitachi S-3400N scanning electron microscope. Cobalt was used as a standard to monitor instrumental drift. An acceleration voltage of 15 kV, a sample current of ∼1 nA, and a counting live time of 80 s was used. The accuracy of the analyses has been confirmed by interlaboratory tests using certified standards (2, 4). Precision of the analyses was typically better than 1 to 4%. Three spots or more were analyzed on each grain, and the average result is used here. Analysis spots were selected away from grain fractures or rims with signs of diagenetic alteration.

Division of Chrome-Spinel Grains into Main Groups.

EC. Grains from equilibrated ordinary chondrites (petrological types 4 to 6) with oxide weight percentages within the ranges of Cr_2O_3: ∼53.0 to 62.0; FeO: ∼23.0 to 32.0; Al_2O_3: ∼4.5 to 8.5; MgO: ∼1.3 to 4.5; V_2O_3: ∼0.55 to 0.95; TiO_2: ∼1.40 to 4.50 (for more extensive discussions, see ref. 1). Small deviations from these values in one or two oxides are marked with red color in the element analyses table (Dataset S1). The FeO values of EC grains can sometimes be lower than 23 wt% because of replacement by MnO and ZnO (see ref. 53). All grains with typical EC composition, but with TiO_2 ≤1.10 wt%, are classified as OtC-V grains. These grains may derive from unequilibrated ordinary chondrites.

Outlier EC. Grains that significantly deviate in MgO, but still can be considered an EC grain are put within Outlier EC categories. These grains may have suffered some diagenetic alteration, but generally V_2O_3 and TiO_2 appear not to have been affected. We divide these grains further into two categories: 1) MgO-depleted grains: Low content of MgO (<1.0 wt%) and usually accompanied by an elevated ZnO content. EC-like grains with <0.5 wt% MgO are classified as OtC-V grains. 2) MgO-enriched grains: High content of MgO >6.0 wt% and usually low (<24 wt%) values of MnO+FeO+ZnO. EC-like grains with MgO >9.0 wt% are classified as OtC-V grains.

OtC-V. Other chrome spinel: that is, grains that do not have the typical equilibrated ordinary chondritic composition, but contain ≥0.45 wt% V_2O_3 and a Cr_2O_3/FeO ratio ≥1.45, indicating a likely meteoritic origin.

OtC. Other chrome-spinel grains, but with V_2O_3 <0.45 wt% or ≥0.45 wt% V_2O_3 together with a Cr_2O_3/FeO ratio <1.45. The OtC grains are likely of terrestrial origin.

The OtC and OtC-V grains are the same as the OC and OC-V grains in our previous papers. The acronyms have been changed in order to avoid confusion with the use of the acronym OC for "ordinary chondrite" in other research. The classification system used here has evolved over time. In single cases in earlier work grains that are at the "border" between two of our present categories may have been put in a different category than in the system applied here. These cases are so rare, however, that they have no bearing on any of the conclusions reached at in the present study.

Division of EC Grains in H, L, and LL Groups. The EC grains can also be divided into the three ordinary chondritic groups—H, L, and LL—using the TiO_2 concentration (2, 10, 54). The average TiO_2 content of the H, L, and LL groups is ∼2.2, 2.7, and 3.4 wt%, respectively. The TiO_2 content follows a Gaussian distribution, with about 10% overlap between the groups. We use the following division: H ≤ 2.50, L = 2.51 to 3.39, and LL ≥ 3.40 wt%, respectively. The exact ranges for dividing grains based on TiO_2 can in principle be arbitrarily set, but they must be used consistently when comparing different time periods. The EC classification into subgroups can also be done with oxygen-3-isotopic analysis, but it has been shown that the TiO_2 approach is as effective as using oxygen isotopes (2, 10, 54). The advantage of using both oxygen isotopes and TiO_2 is that uncertainties from compositional overlaps in respective approach can be resolved in greater detail. In practice, however, isotope and element overlaps tend to cancel each other out, therefore using both methods instead of only TiO_2 will not significantly affect the division of the grains. The ~10% overlap in TiO_2 content between the three groups is insignificant when each of the three groups has similar abundances, but when one group strongly dominates, such as the L chondrites after the LCPB break-up, the overlap creates false high numbers of grains in the other groups. We therefore present our data corrected for a 10% overlap in TiO_2 concentrations between groups.

When comparing chromite TiO_2 results between different time windows, the sample sizes vary, which may cause considerable uncertainties, especially for time windows with small number of analyses. In order to compare time windows in a meaningful way, the statistical uncertainty associated with the number of analyses has been estimated (Fig. 3). The probability that an EC grain in a time window belongs to one of three populations can be evaluated through the classical binomial probability equation (55). The detection limit (X_L) is dependent upon both the confidence level assigned (p_L) and the total number of grains analyzed (n) in each time window: $X_L = 1 - (1- p_L)1/n$. Only populations exceeding the detection limit were believed to be a statistically important constituent of the population and valid for further discussion. The expected uncertainty is illustrated as a function of relative abundance of the subgroup population (X_i) and the total number of grains analyzed (n) in a specific time window: $2\sigma i = 2\sqrt{nXi(1-Xi)}$.

Calculation of Flux (Grains m^{-2} ka^{-1}). The extraterrestrial flux (EF) is here expressed as the number of EC-grains of a specific size fraction deposited within a square meter during a time span of 1,000 y. Variables are sedimentation rate (*SR*) and number of grains per kilogram of rock (*N*). Constants are the area of deposition and the density of limestone (ρ). The flux equation reads as follows: $EF = 100 \times 100 \times SR \times \rho \times N$, where *SR* is expressed as centimeters per 1,000 y, *N* is expressed as grains per kilogram of rock, and ρ is expressed as gram per cubic centimeter of rock. For compilation of data for all windows and discussion on the flux parameters, see *SI Appendix*, *SI Text* and Tables S1 and S2.

Data Availability. All study data are included in the article and supporting information.

ACKNOWLEDGMENTS. We thank Edward Anders for encouragement, discussions, and comments on an earlier draft; Ellinor Martin for providing the additional results for one of the Late Cretaceous time windows; Knut Deppert, Per Eriksson, and Per Kristiansson for making the study possible at Lund University; Shiyong Liao for providing helpful comments on error estimates; Faisal Iqbal for assisting in the laboratory; and three anonymous reviewers for comments that improved the manuscript. Support during field work was provided by Federico Oloriz and Victoriano Pujalte in Spain, Luca Martiri in Italy, and Samuele Boschi in Sweden. The project was funded by the Knut and Alice Wallenberg Foundation, Swedish Research Council and European Research Council (Advanced Grant ASTROGEOBIOSPHERE).

1. B. Schmitz, Extraterrestrial spinels and the astronomical perspective on Earth's geological record and evolution of life. *Chem. Erde* **73**, 117–145 (2013).
2. B. Schmitz *et al*., The meteorite flux to Earth in the Early Cretaceous as reconstructed from sediment-dispersed extraterrestrial spinels. *Geology* **45**, 807–810 (2017).
3. E. Martin, B. Schmitz, H.-P. Schönlaub, From the mid-Ordovician into the Late Silurian: Changes in the meteorite flux after the L-chondrite parent breakup. *Meteorit. Planet. Sci.* **53**, 2541–2557 (2018).
4. B. Schmitz *et al*., The micrometeorite flux to Earth during the Frasnian–Famennian transition reconstructed in the Coumiac GSSP section, France. *Earth Planet. Sci. Lett.* **522**, 234–243 (2019).
5. E. Martin, B. Schmitz, A. Montanari, A record of the micrometeorite flux during an enigmatic extraterrestrial ^{3}He anomaly in the Turonian (Late Cretaceous). *Spec. Pap. Geol. Soc. Am.* **542**, 303–318 (2019).
6. W. F. Bottke *et al*., "The collisional evolution of the main asteroid belt" in *Asteroids IV*, P. Michel, F. E. DeMeo, W. F. Bottke, Eds. (University of Arizona Press, 2015), pp. 701–724.
7. R. C. Greenwood, T. H. Burbine, I. A. Franchi, Linking asteroids and meteorites to the primordial planetesimal population. *Geochim. Cosmochim. Acta* **277**, 377–406 (2020).
8. F. E. DeMeo, B. Carry, Solar System evolution from compositional mapping of the asteroid belt. *Nature* **505**, 629–634 (2014).
9. D. Nesvorný, D. Vokrouhlický, W. F. Bottke, M. Sykes, Physical properties of asteroid dust bands and their sources. *Icarus* **181**, 107–144 (2006).
10. P. R. Heck *et al*., Rare meteorites common in the Ordovician period. *Nat. Astron.* **1**, 35 (2017).
11. P. W. Reiners, A. V. Turchyn, Extraterrestrial dust, the marine lithologic record, and global biogeochemical cycles. *Geology* **46**, 863–866 (2018).
12. D. Nesvorný, M. Broz, V. Carruba, "Identification and dynamical properties of asteroid families" in *Asteroids IV*, P. Michel, F. E. DeMeo, W. F. Bottke, Eds. (University of Arizona Press, 2015), pp. 297–321.
13. F. Spoto, A. Milani, Z. Knežević, Asteroid family ages. *Icarus* **257**, 275–289 (2015).
14. P. Paolicchi, F. Spoto, Z. Knežević, A. Milani, Ages of asteroid families estimated using the YORP-eye method. *Mon. Not. R. Astron. Soc.* **484**, 1815–1828 (2019).
15. S. Marchi *et al*., High-velocity collisions from the lunar cataclysm recorded in asteroidal meteorites. *Nat. Geosci.* **6**, 303–307 (2013).
16. F. Marzari *et al*., Origin and evolution of the Vesta asteroid family. *Astron. Astrophys.* **316**, 248–262 (1996).
17. P. Schenk *et al*., Compositional control on impact crater formation on mid-sized planetary bodies: Dawn at Ceres and Vesta, Cassini at Saturn. *Icarus* **359**, 114343 (2021).
18. B. Schmitz *et al*., An extraterrestrial trigger for the mid-Ordovician ice age: Dust from the breakup of the L-chondrite parent body. *Sci. Adv.* **5**, eaax4184 (2019).
19. The Meteoritical Society, The Meteoritical Bulletin Database https://www.lpi.usra.edu/meteor/metbull.php. Accessed 19 May 2020.
20. A. Milani, Z. Knežević, F. Spoto, P. Paolicchi, Asteroid cratering families: Recognition and collisional interpretation. *Astron. Astrophys.* **622**, 1–18 (2019).
21. W. F. Bottke, D. Vokrouhlický, D. Nesvorný, An asteroid breakup 160 Myr ago as the probable source of the K/T impactor. *Nature* **449**, 48–53 (2007).
22. V. Reddy *et al*., Chelyabinsk meteorite explains unusual spectral properties of Baptistina asteroid family. *Icarus* **237**, 116–130 (2014).
23. J. R. Masiero, A. K. Mainzer, T. Grav, J. M. Bauer, R. Jedicke, Revising the age for the Baptistina asteroid family using WISE/NEOWISE data. *Astrophys. J.* **759**, 14 (2012).
24. M. J. Dykhuis, L. Molnar, S. J. Van Kooten, R. Greenberg, Defining the Flora family: Orbital properties, reflectance properties and age. *Icarus* **243**, 111–128 (2014).
25. B. Schmitz *et al*., A new type of solar-system material recovered from Ordovician marine limestone. *Nat. Commun.* **7**, s11851 (2016).
26. S. Boschi, B. Schmitz, E. Martin, F. Terfelt, The micrometeorite flux to Earth during the earliest Paleogene reconstructed in the Bottaccione section (Umbrian Apennines) Italy. *Meteorit. Planet. Sci.* **55**, 1615–1628 (2020).
27. M. Schmieder, D. A. Kring, Earth's impact events through geologic time. A list of recommended ages for terrestrial impact structures and deposits. *Astrobiology* **20**, 91–141 (2020).
28. E. Anders, Origin, age and composition of meteorites. *Space Sci. Rev.* **3**, 583–714 (1964).
29. K. Keil, H. Haack, E. R. D. Scott, Catastrophic fragmentation of asteroids: Evidence from meteorites. *Planet. Space Sci.* **42**, 1109–1122 (1994).
30. D. D. Bogard, K-Ar ages of meteorites: Clues to parent-body thermal histories. *Chem. Erde* **71**, 207–226 (2011).
31. T. D. Swindle, D. A. Kring, J. R. Weirich, $^{40}Ar/^{39}Ar$ ages of impacts involving ordinary chondrite meteorites. *Geol. Soc. Lond. Spec. Publ.* **378**, 333–347 (2013).
32. K. A. Farley, Late Eocene and late Miocene cosmic dust events: Comet showers, asteroid collisions or lunar impacts? *Spec. Pap. Geol. Soc. Am.* **452**, 27–35 (2009).
33. K. A. Farley, A. Montanari, R. Coccioni, A record of the extraterrestrial ^{3}He flux through the Late Cretaceous. *Geochim. Cosmochim. Acta* **84**, 314–328 (2012).
34. S. Mukhopadhyay, K. A. Farley, A. Montanari, A 35 Myr record of helium in pelagic limestone from Italy: Implications for interplanetary dust accretion from the early Maastrichtian to the middle Eocene. *Geochim. Cosmochim. Acta* **65**, 653–669 (2001).
35. S. Boschi *et al*., Late Eocene ^{3}He and Ir anomalies associated with ordinary chondritic spinels. *Geochim. Cosmochim. Acta* **204**, 205–218 (2017).
36. S. Boschi, B. Schmitz, A. Montanari, Distribution of chrome-spinel grains across the ^{3}He anomaly of the Tortonian Stage at the Monte dei Corvi section, Italy. *Spec. Pap. Geol. Soc. Am.* **542**, 383–391 (2019).
37. P. Farinella, D. Vokrouhlický, A. Morbidelli, "Delivery of material from the asteroid belt" in *Accretion of Extraterrestrial Matter Throughout Earth's History*, B. Peucker-Ehrenbrink, B. Schmitz, Eds. (Kluwer, New York, 2001), pp. 31–49.
38. S. J. Kortenkamp, S. F. Dermott, D. Fogle, K. Grogan, "Sources and orbital evolution of interplanetary dust accreted by Earth" in *Accretion of Extraterrestrial Matter Throughout Earth's History*, B. Peucker-Ehrenbrink, B. Schmitz, Eds. (Kluwer, New York, 2001), pp. 13–30.
39. J. A. Burns, P. L. Lamy, S. Soter, Radiation forces on small particles in the solar system. *Icarus* **40**, 1–48 (1979).
40. A. Meibom, B. E. Clark, Evidence for the insignificance of ordinary chondritic material in the asteroid belt. *Meteorit. Planet. Sci.* **34**, 7–24 (1999).
41. P. Vernazza *et al*., Compositional differences between meteorites and near-Earth asteroids. *Nature* **454**, 858–860 (2008).
42. P. Vernazza, B. Zanda, T. Nakamura, E. Scott, S. Russell, "The formation and evolution of ordinary chondrite parent bodies" in *Asteroids IV*, P. Michel, F. E. DeMeo, W. F. Bottke, Eds. (University of Arizona Press, 2015), pp. 617–634.
43. S. F. Dermott, A. A. Christou, D. Li, T. J. J. Kehoe, J. M. Robinson, The common origin of family and non-family asteroids. *Nat. Astron.* **2**, 549–554 (2018).
44. P. G. Brown *et al*., The Hamburg meteorite fall: Fireball trajectory, orbit, and dynamics. *Meteorit. Planet. Sci.* **54**, 2027–2045 (2019).
45. P. Vernazza *et al*., Multiple and fast: The accretion of ordinary chondrite parent bodies. *Astrophys. J.* **791**, 120 (2014).
46. J. W. Noonan *et al*., Search for the H chondrite parent body among the three largest S-type asteroids: (3) Juno, (7) Iris, (25) Phocaea. *Astron. J.* **158**, 213 (2019).
47. D. Nesvorný, D. Vokrouhlický, A. Morbidelli, W. F. Bottke, Asteroidal source of L chondrite meteorites. *Icarus* **200**, 698–701 (2009).
48. A. M. McGraw, V. Reddy, J. A. Sanchez, Do L chondrites come from the Gefion family? *Mon. Not. R. Astron. Soc.* **476**, 630–634 (2018).

49. M. M. M. Meier *et al*., Park Forest (L5) and the asteroidal source of shocked L chondrites. *Meteorit. Planet. Sci.* **52**, 1561–1576 (2017).
50. J. Wisdom, Meteorite transport—Revisited. *Meteorit. Planet. Sci.* **55**, 766–770 (2020).
51. S. K. Fieber-Beyer, M. J. Gaffey, Near-infrared spectroscopy of 3:1 Kirkwood Gap asteroids III. *Icarus* **257**, 113–125 (2015).
52. R. Wieler, T. Graf, "Cosmic ray exposure history of meteorites" in *Accretion of Extraterrestrial Matter Throughout Earth's History*, B. Peucker-Ehrenbrink, B. Schmitz, Eds. (Kluwer, New York, 2001), pp. 221–240.
53. B. Schmitz, M. Tassinari, B. Peucker-Ehrenbrink, A rain of ordinary chondritic meteorites in the early Ordovician. *Earth Planet. Sci. Lett.* **194**, 1–15 (2001).
54. P. R. Heck *et al*., A search for H-chondritic chromite grains in sediments that formed immediately after the breakup of the L-chondrite parent body 470 Ma ago. *Geochim. Cosmochim. Acta* **177**, 120–129 (2016).
55. D. Zwillinger, *CRC Standard Mathematical Tables and Formulae* (Chapman & Hall/CRC, Boca Raton, 2003).
56. S. Liao, M. H. Huyskens, Q.-Z. Yin, B. Schmitz, Absolute dating of the L-chondrite parent body breakup with high-precision U-Pb zircon geochronology from Ordovician limestone. *Earth Planet. Sci. Lett.* **547**, 116442 (2020).
57. E. Martin, B. Schmitz, W. Alvarez, L. Aguirre-Palafox, F. Terfelt, Chemistry of sediment-dispersed chrome-spinel grains from the Early Cretaceous (Albian/Aptian) Calera Limestone, Pacifica Quarry, California. (Pangaea, 2020) https://doi.pangaea.de/10.1594/PANGAEA.920972. Accessed 25 August 2020.
58. C. Alwmark, B. Schmitz, The origin of the Brunflo fossil meteorite and extraterrestrial chromite in mid-Ordovician limestone from the Gärde quarry (Jämtland, central Sweden). *Meteorit. Planet. Sci.* **44**, 95–106 (2009).